frontiers | Frontiers in Astronomy and Space Sciences

TYPE Brief Research Report
PUBLISHED 01 August 2023
DOI 10.3389/fspas.2023.1064368

OPEN ACCESS

EDITED BY
Joseph E. Borovsky,
Space Science Institute, United States

REVIEWED BY
Bengt Eliasson,
University of Strathclyde, United Kingdom
Paul Bernhardt,
University of Alaska Fairbanks, United States

*CORRESPONDENCE
Brett Isham,
brettisham@gmail.com

†PRESENT ADDRESS
Fourth State Communications, LLC, Cheyenne, WY, United States

RECEIVED 08 October 2022
ACCEPTED 30 May 2023
PUBLISHED 01 August 2023

CITATION
Isham B, Bullett T, Gustavsson B, Polisensky E, Brum C, Fallen C, Belyey V, Parra-Rojas F, Norouzi L, Stramkals A and Ökten MB (2023), Science goals for a high-frequency radar and radio imaging array.
Front. Astron. Space Sci. 10:1064368.
doi: 10.3389/fspas.2023.1064368

Science goals for a high-frequency radar and radio imaging array

Brett Isham[1]*, Terence Bullett[2], Björn Gustavsson[3], Emil Polisensky[4], Christiano Brum[5], Christopher Fallen[6†], Vasyl Belyey[7], Francisco Parra-Rojas[8], Leila Norouzi[9], Arturs Stramkals[10] and Mehmet Baran Ökten[11]

[1]Electrical and Computer Engineering, Interamerican University of Puerto Rico, Bayamón, PR, United States, [2]Cooperative Institute for Research in Environmental Sciences, University of Colorado, Boulder, CO, United States, [3]Department of Physics and Technology, University of Tromsø, Tromsø, Norway, [4]Remote Sensing Division, U.S. Naval Research Laboratory, Washington, DC, United States, [5]Arecibo Observatory, University of Central Florida, Arecibo, PR, United States, [6]Space Vehicles Directorate, U.S. Air Force Research Laboratory, Albuquerque, NM, United States, [7]Private Researcher, Oslo, Norway, [8]Department of Natural Sciences and Mathematics, Interamerican University of Puerto Rico, Bayamón, PR, United States, [9]Private Researcher, Seattle, WA, United States, [10]Department of Physics and Astronomy, Uppsala University, Uppsala, Sweden, [11]Department of Metallurgical and Materials Engineering, Yildiz Technical University, Istanbul, Türkiye

A medium and high-frequency antenna array for radar and radio imaging of the ionosphere is planned for installation in Aguadilla, Puerto Rico. Science goals include the study of space weather, radio propagation, meteors, lightning, and plasma physics. Radio imaging is ideal for the study of stimulated ionospheric radio emissions, such as those induced by the Arecibo Observatory high-power HF radio transmitter, which is likely to be restored to operation in the near future. The array will be complemented by a wide variety of instruments fielded by collaborators, and will be a rich source of student projects at all levels.

KEYWORDS

space weather, plasma irregularities and turbulence, stimulated electromagnetic emissions, high frequency radio and radar imaging, radio scattering and polarization, orbital angular momentum, solar radar, Arecibo Observatory

1 Introduction

A 2 to 25-MHz radar and radio imaging array is proposed to be installed at the site of the former U.S. Air Force Ramey Solar Observatory in Aguadilla in northwest Puerto Rico. The main array will consist of 64 4-m crossed active antenna elements arranged within a 400-m-diameter area. Sixteen relocatable cableless receivers will also be included, the phases of which will be maintained through the use of GPS-disciplined rubidium clocks. The cableless elements may be used independently, or together with the main array for improved imaging resolution. Radar imaging will be done in collaboration with the high-frequency (HF) radar system at the United States Geological Survey (USGS) San Juan Observatory in Cayey, Puerto Rico, 110 km east-southeast of Aguadilla. In the future an HF radar transmitter may be also be installed in Aguadilla.

2 Research

Research areas to which the radio array can be applied include space weather, ionospheric structure and dynamics, plasma turbulence, stimulated radio emissions, radio wave propagation and scattering, lightning, meteors, and the development of new radio technologies. Imaging and multisite measurements in the medium and high-frequency bands require the incorporation of ionospheric propagation effects into the analysis algorithms, which will motivate new developments in remote sensing and radio imaging. Direction of arrival and imaging measurements made by the array will improve our understanding of how space plasmas interact with the Earth's magnetic field under disturbed conditions, which are the conditions most disruptive to communications and navigation signals. The science goals of the array are described in more detail below.

2.1 Space weather

The antenna array will be used as an imaging radar receiver for transmissions from the HF Vertical Incidence Pulsed Ionospheric Radar (VIPIR) in Cayey, Puerto Rico, for studies of phenomena such as atmospheric gravity waves, plasma irregularities, and space weather monitoring (Grubb et al., 2008). These observations would complement past observations made by the Cayey HF and Arecibo 430-MHz radars, such as those shown in **Figure 1**, with mesoscale radar images of the ionosphere surrounding and in-between the Cayey and Arecibo instruments. In the same way, radar imaging can be used to supplement airglow imagers, providing a different view of the same geographic regions and also operating through gaps in airglow data during the day and on cloudy nights. The array might also be used for space weather studies in a passive imaging mode as an interferometric riometer (McKay et al., 2015), and scintillation measurements could provide additional data on ionospheric irregularities and structure (Booker et al., 1987; Booker and Tao, 1987).

2.2 Natural plasma turbulence

Plasma turbulence is part of the small-scale physical foundation of space weather. If we can better understand the fundamental processes that drive plasma turbulence, we will be able to better understand space weather as well. Ionospheric plasma turbulence may be divided into two categories: natural and artificially stimulated. Natural turbulence involves microscopic processes directly related to space weather. Stimulated turbulence involves the same microscopic processes but is controllable through the use of high-power transmitting, or heating, facilities (Grach et al., 2016; Streltsov et al., 2018; Yampolski et al., 2019), and this capability can be used to better understand natural turbulence. The radar and radio imaging array discussed here is designed to allow in-depth studies of both kinds of turbulence.

2.3 Artificial plasma turbulence and stimulated radio emissions

High-power, high-frequency ionospheric research transmitters capable of creating artificial ionospheric turbulence are operated at the High-Frequency Active Auroral Research Program (HAARP) observatory in Gakona, Alaska, at the European Incoherent Scatter Scientific Association (EISCAT) observatory in Tromsø, Norway, at the Sura observatory in Vasilsursk, Russia, and, until 2020, and, likely again in the near future, at Arecibo Observatory in Arecibo, Puerto Rico (Streltsov et al., 2018; Ferguson et al., 2022). Artificial ionospheric turbulence produces stimulated ionospheric radio emissions (also known as stimulated electromagnetic emissions or SEE), which share many characteristics with natural radio emissions (Thidé et al., 1982; Leyser, 2001; LaBelle and Treumann, 2002; LaBelle, 2012; Sergeev et al., 2013; Eliasson et al., 2021). Many spectral features have been identified, and some have been associated with specific plasma processes. Much attention has been paid to the heights of the emission regions, however, little work has been done in regard to the horizontal locations of the emissions, or to their geometrical or geographic relation to the geomagnetic field and to each other. High-frequency radio waves reflect or refract not only at different heights, but at different horizontal offsets (Rietveld et al., 1993). Different spectral features, due to differing plasma processes, might be expected to occur not only at different altitudes, but with different spatial distributions, for example, at different horizontal offsets relative to the geomagnetic zenith, i.e., roughly in the north-south direction (Isham et al., 2005; Tereshchenko et al., 2006). **Figure 2** and **Figure 3** show that simple HF radio interferometric methods are sensitive enough to detect changes in the locations of SEE source regions. The array will extend that technique to multiple antennas with multiple baselines, which can then be used for imaging of the emission region.

Radio imaging of artificially-stimulated radio emissions would be transformative. Images of the structure of stimulated radio emissions from the radio/plasma interaction region will help in determining the exact geometries of the source regions of the many radio spectral features with respect to the geomagnetic field. In addition, radio images at each polarization (O and X) for each emission feature could be constructed (Carozzi et al., 2001). Turbulence at high latitudes is known to be dependent on the longitudinal aspect angle with respect to the geomagnetic field, and this could be studied through radio imaging using the array (Isham et al., 2005). A variety of observations of stimulated radio emissions from Arecibo have been done using previous Arecibo HF transmitters (Thidé et al., 1989; Thidé et al., 1995; Mahmoudian et al., 2019). The array discussed here will be capable of much higher time and frequency resolution than could previously be measured.

The antenna elements of the array will be active crossed electric dipoles, and so will be capable of making a separate image in each polarization, which for ionospheric emissions would be the two circular polarizations, O and X. Very little work has been done on the polarization of stimulated ionospheric emissions, but the available

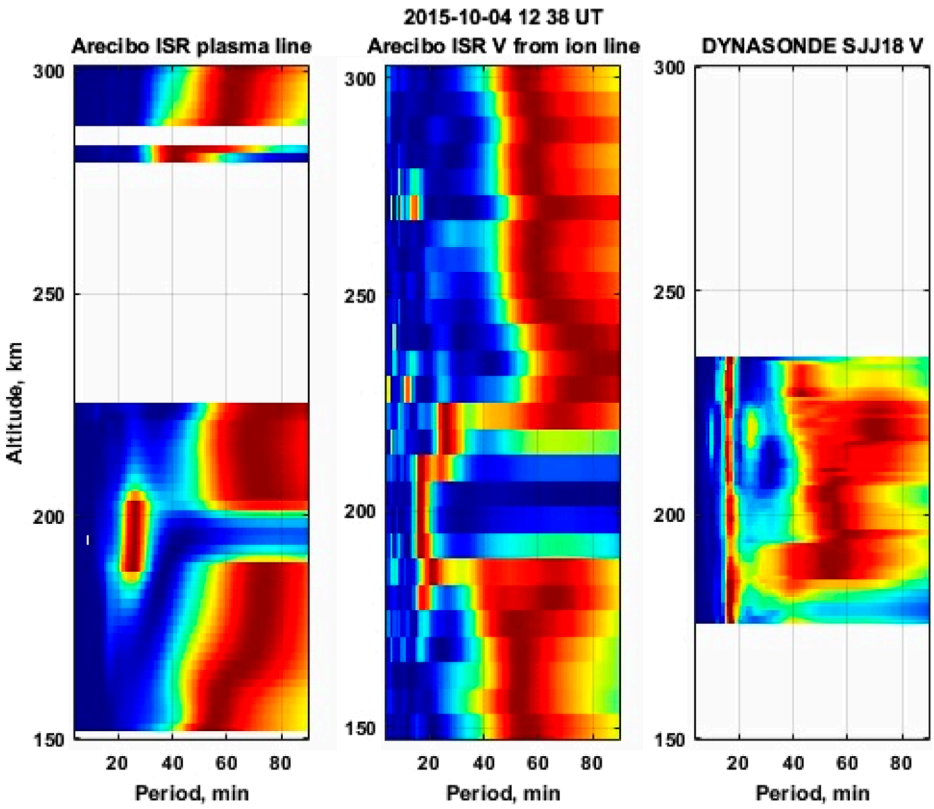

FIGURE 1
Measurements of waves in the thermosphere above Arecibo and Cayey, Puerto Rico. Lomb-Scargle periodograms are shown of the dimensionless amplitudes of variations in selected plasma parameters, with blue smallest and red largest, vs. period and altitude (Zabotin et al., 2016), as follows: Left panel: Variations in plasma frequency over Arecibo derived from 430-MHz incoherent scatter radar plasma line measurements. Middle panel: Variations in vertical velocity over Arecibo derived from 430-MHz incoherent scatter radar ion line measurements. Right panel: Variations in vertical velocity over Cayey derived from HF radar observations using the dynamic sounding (Dynasonde) technique (Zabotin et al., 2006). The white areas indicate altitudes with no data due to instrumental limitations; these areas are different in each panel since different instruments and different measurement methods, each with different limitations, were used to obtain the data. Note also that the Arecibo plasma line and ion line panels show the variations of different parameters, which explains in part why the structures shown in the data are not exactly aligned. The Cayey and Arecibo radars are 70 km apart, yet the similarities in the data clearly show that the same phenomena are being observed by each. Through the use of radar imaging at a variety of HF frequencies, a time series of images of these waves as a function of altitude may be obtained in the ionosphere between Arecibo and Cayey. This figure is reproduced from the supplementary material of Zabotin et al. (2016), who emphasize that this is just one instance of a 10-h dataset, and that the entire dataset should be considered to correctly interpret the results.

results indicate that the different spectral features likely have distinct polarization properties (see the left panel of **Figure 4**). Polarization data might also be applied to the study of possible orbital angular momentum (OAM) modes in the received emissions (see the right panel **Figure 4**). The ability to routinely measure the polarization images of the stimulated radio signals will almost certainly lead to new and unexpected discoveries.

The imaging and polarization capabilities of the array promise to significantly advance our understanding of these little-studied aspects of stimulated radio emissions. At the longer wavelengths, where imaging is not feasible, the phase coherence of the radio receivers of the array allows radio direction-finding to be used. Direction-finding of stimulated radio emissions from the ionosphere (Isham et al., 2005; Tereshchenko et al., 2006) (see **Figures 2**, **3**) has not yet been done at mid or low latitudes.

Radio imaging and direction-finding measurements can be complemented through the placement of the relocatable receivers of the array on long baselines to the east or west, for example, in eastern Puerto Rico or on nearby islands. This can provide a variety of oblique perspective angles from which to observe the radio emissions. Variations in the properties of the radio emissions as a function of observing angle would provide additional clues useful in the unraveling of turbulent processes, as the radiation pattern of the emissions is determined by ionospheric currents driven by those processes.

The second harmonic and subharmonics of stimulated radio emissions have been observed on limited occasions in the past (Karashtin et al., 1986; Derblom et al., 1989; Blagoveshchenskaya et al., 1998). The Arecibo HF transmitter most recently operated at two frequencies, 5.1 and 8.175 MHz; the receivers of the array will allow observations of radio emission harmonics of those frequencies up to the fourth or fifth at 5.1 MHz and third at 8.175 MHz, and also of subharmonics. Measurements of harmonic and subharmonic emissions may shed light on the emission mechanisms by either verifying or constraining emission theories and models.

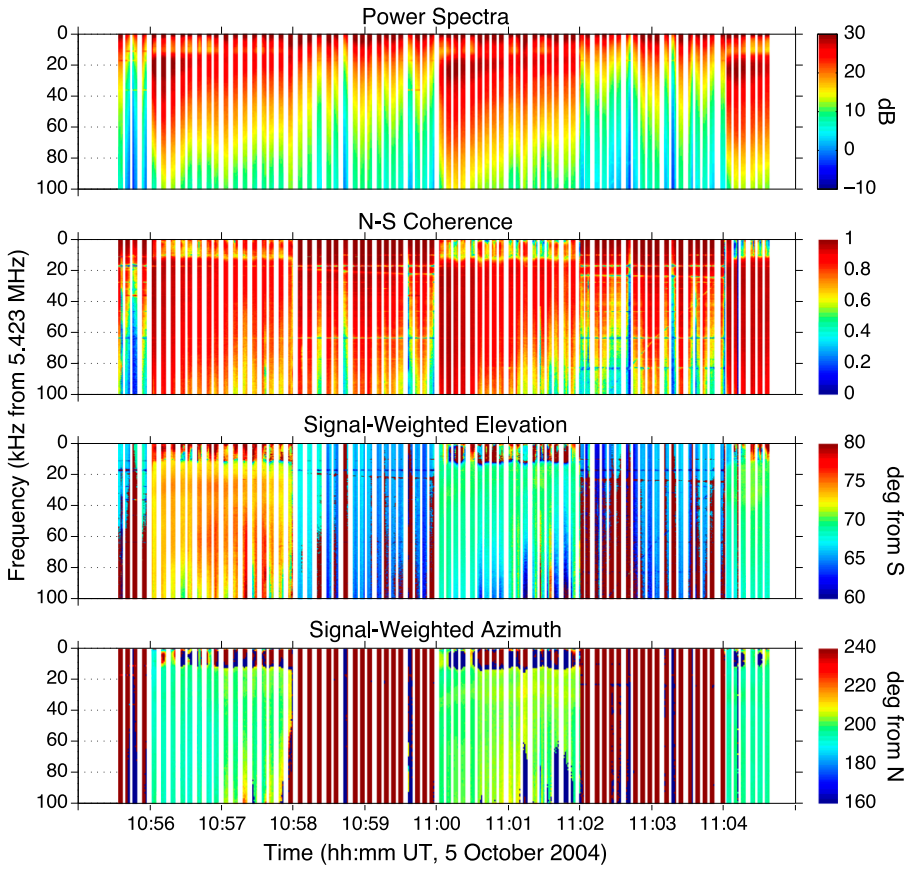

FIGURE 2
Direction angles of artificially-stimulated "broad upshifted maximum 1" (BUM1) radio emissions computed from raw voltage interferometer data taken on 5 October 2004 near Tromsø, Norway (Isham et al., 2005). The BUM1 can be seen between about 15 and 100 kHz relative to the pump frequency. The elevation angle of the BUM1 is about 74° during the first pump cycle and about 70° during the following two cycles, corresponding to 3° and 7° south of field-aligned. Elevation and azimuth were computed from the north-south and east-west antenna cross phases. The HF beam was centered on 14.0° south during the first on period and on 17.5° south during the second and third on periods. The HF pump was on for 2 min every 4 min; two complete and one partial on periods are shown, from 10:56 to 0:58 UT, from 11:00 to 11:02 UT, and beginning at 11:04 UT; this can be seen in all four panels, but is most distinct in the bottom panel. Time and frequency resolutions are 1 s and 1 kHz. The white areas within the panels, most of which appear as thin vertical white stripes, are times with missing data, primarily due to a technical fault in the recording system. Figure modified from figure 13 of Isham et al. (2005).

An interesting and related topic is the search for the two-plasmon decay instability (Kruer, 1990; DuBois, 2000; Russell and DuBois, 2001; DuBois et al., 2011). To search for two-plasmon decay, the HF transmission frequency should ideally be chosen to be greater than the peak F-region frequency, and the receiving instrument tuned to one-half and three-halves of the transmitted value. Oblique radio emissions, as discussed above, are also thought to be a possible diagnostic for two-plasmon decay (Meyer and Zhu, 1993). While there has been extensive theoretical work on the mechanisms of a variety of SEE features, including the broad upshifted maximum (BUM), the downshifted maximum (DM), and the narrow continuum (NC) (Cheung et al., 1998; Mjølhus, 1998; Eliasson et al., 2012; Sergeev et al., 2013; Grach et al., 2016; Streltsov et al., 2018), there is much room for improvement in our understanding of the emission processes. In particular, to date there is no predictive theory of electromagnetic radio emissions such as exists for the electrostatic plasma waves that typically accompany them (Cheung et al., 2001; DuBois et al., 2001). Measurements made with the imaging radio array discussed here will assist in improving existing models.

2.4 High-frequency radio wave propagation

Because of the refractive properties of the ionosphere at high frequencies, the radio imaging techniques discussed here give apparent direction of arrival of the signals being imaged. To obtain the true directions, HF wave propagation must be taken into account. HF propagation codes, also known as ray tracing codes, along with observations and models of the profile and structure of the ionosphere, may be used as needed to correct images and arrival angles for distortions caused by the ionosphere (Henderson et al., 2022). Density profile information for ray tracing calculations may be obtained from the instrument cluster operating on Culebra Island, Puerto Rico (PI Dr. Pedrina Terra), from the Digisonde and VIPIR HF radars operating in Cayey, Puerto Rico (PI Dr. Terence

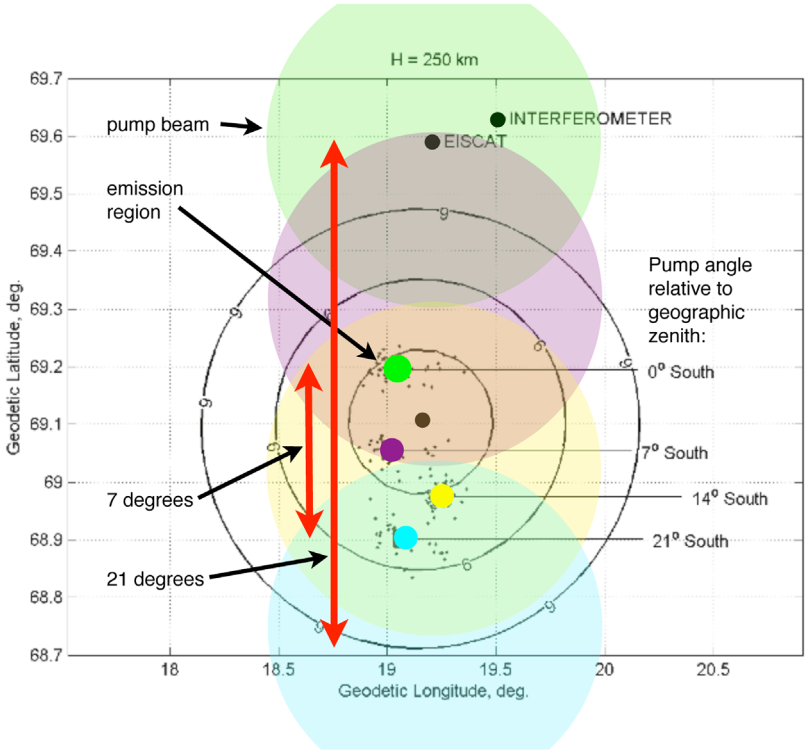

FIGURE 3
Direction angles of artificially-stimulated "downshifted peak" (DP) radio emissions computed from raw voltage interferometer data taken on 6 October 2004 near Tromsø, Norway (Tereshchenko et al., 2006). The emissions were stimulated by an HF pump beam at 4.04 MHz. Vertical pump beam pointing began at 15:30 UT, 7° south at 15:34 UT, 14° south at 15:38 UT, and 21° south at 15:42 UT, corresponding to 13° north, 6° north, 1° south, and 8° south of field-aligned. The large colored circles show HF beam positions, while the matching small colored circles show corresponding mean locations of the radio emissions. The field-aligned position is located at the center of the solid-line contours, which give the angle between the pump beam direction and the geomagnetic field at 250 km. The location of the DP emission maximum is clearly influenced by the direction of the pump beam, but, for each pump direction, the emission region remains closer to a fixed angular location than to the angle of the pump. This hints at the role of the geomagnetic field in the emission process, which could be further studied using radio imaging. Figure modified from figure 8 of Tereshchenko et al. (2006).

Bullett), and from instruments to be installed by collaborators alongside the array in Aguadilla, Puerto Rico. Ionospheric models may be used to help fill in data gaps. In addition, as previously mentioned, it is likely that the Arecibo HF transmitter will be restored to operation (Ferguson et al., 2022). If so, the Arecibo optical imagers and lidars could continue in operation. With relatively little additional work, an ionosonde could be installed at the Arecibo site or nearby, and the Arecibo 430-MHz radar could be restored and restarted.

2.5 Microphysics of high-frequency radio wave scattering

There is a long-standing discussion about the physics of high-frequency radio wave scattering from the ionospheric plasma and the optimal way to process measurements of the scattered waves. One of the measurement methods used is known as the dynamic sounding, or Dynasonde, technique. A fundamental strategy of the Dynasonde technique is the use of individual echoes, detected without averaging the data from multiple transmitted pulses, as is frequently done by other methods (Wright and Pitteway, 1979; Wright et al., 1980; Sedgemore et al., 1998; Reinisch et al., 2005; Bertoni et al., 2006; Zabotin et al., 2006; Reinisch et al., 2009; Paznukhov et al., 2012). During Dynasonde data processing, it has been noted that an echo detected on a given pulse may frequently be seen again on the following pulse, suggesting that the sources of the individual echoes are deterministic structures and not random. However, dynamic sounding relies on direction-finding, without the angular resolution that radio imaging techniques may provide, so that it is not possible to say whether a given Dynasonde echo is from a defined and well-located structure or due to a geometric average of the scattering from one or more extended structures. One way to study this process would be to compare radar aperture synthesis images made using the radio array with the locations of particular echoes measured by the Dynasonde technique.

2.6 Lightning

Aguadilla is located north of the rugged hills of central Puerto Rico, where many thunderclouds form and pass overhead, frequently undergoing electrical activity while doing so. The radio array discussed here can be used as a lightning interferometer capable of locating the positions of tens of thousands of discrete radio emission sources from a single flash of lightning (Stock et al.,

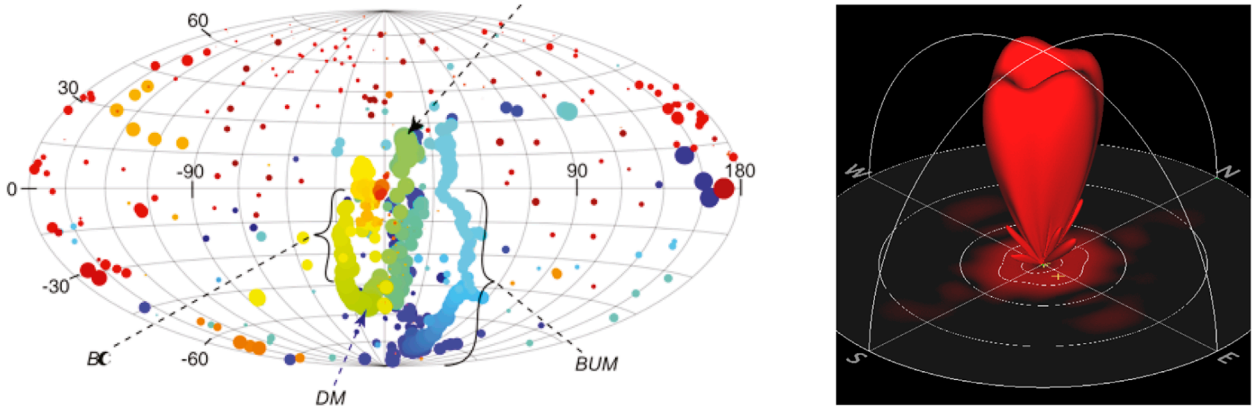

FIGURE 4
Left panel: Polarization of stimulated radio emission spectral features, measured at the Sura observatory in Russia using crossed electric dipoles, and plotted on the Poincaré sphere (Carozzi et al., 2001). The array will be capable of making an image of the radio emissions in each circular polarization, as a function of frequency and time. Copied from plate 1 of Carozzi et al. (2001). Right panel: Radio phase mode beam (OAM l =1) transmitted from the HAARP observatory in Alaska (Leyser et al., 2009). Diagram courtesy of Thomas Leyser. Although unambiguous detection of OAM modes requires three-axis field information, careful measurement of the phase differences in the received waves at widely separated locations may yield clues to possible OAM content of the received waves (Mohammadi et al., 2010a; Mohammadi et al., 2010b).

2014; Hare et al., 2018), and to study medium and high-frequency electromagnetic radio emissions due to collisions between sprite streamers (Garnung et al., 2021). These capabilities would dramatically complement the types of thunderstorm measurements that were made using the previous Arecibo 430-MHz and 46.8-MHz radars (Holden et al., 1986; Chilson et al., 1993). Measurements of lightning emissions by the radio array may also be used to compute rapid ionograms using the ionospheric reflections of the emissions (Obenberger et al., 2018).

2.7 Meteors

The array may be used for radar and radio observations of meteors, which would complement past observations of meteors made by the Arecibo Observatory 430-MHz and 46.8-MHz radars (Holden et al., 1986; Chilson et al., 1993; Isham et al., 2000; Obenberger et al., 2020).

2.8 Development of new radio technologies

The multiple, phase-coherent measurement channels of the array could be used to develop the full-polarization capabilities of vector antennas, both singly and in small arrays, of interest in radio communications and radar and radio remote sensing, and in the study of radio or electromagnetic orbital angular momentum (OAM), also known as radio phase modes. Orbital angular momentum has been studied extensively in the optical frequency range and has relatively recently come into the area of active research in radio frequencies (Thidé et al., 2007; Mohammadi et al., 2010a; Mohammadi et al., 2010b). Careful measurement of the phase differences in the received waves at widely separated locations, as would be possible using the distributed polarization measurement capabilities of the array, can also yield clues to possible OAM content (Mohammadi et al., 2010a; Mohammadi et al., 2010b). The previous Arecibo high-power HF transmitter had a three-point transmitting geometry that could be phased to transmit OAM modes ±1, although not pure modes due to the limited number of transmitting elements. This would likely also be possible, and even improved, in a restored Arecibo high-power HF transmitter (Ferguson et al., 2022) (see the right panel **Figure 4**).

In addition to vector antennas, the flexibility of the array allows exploration of other antenna designs and radio techniques, both at HF and higher frequencies. For optimal compatibility and performance with the Cayey and Arecibo transmitters, the primary receiver frequencies are optimized between 2 and 25 MHz. However, an alternate input allows the receivers of the array to operate down to 0.1 MHz and unaliased up to 60 MHz, and aliased up to 400 MHz. Thus, with some additional preparation and using suitable antennas, signals at other frequencies may be received. For example, at frequencies above 50 MHz, passive radar techniques might be developed using existing FM and digital television transmitters (Meyer and Sahr, 2004; Mir and Sahr, 2007; Vertatschitsch, 2013).

3 Education

The radio array may be used in a wide range of inspiring student projects, such as measuring the local radio environment, mapping the radio sky, analysis of radar soundings and directional measurements, development of improved radar and radio imaging, design and use of vector antennas, and implementation of passive radar. For example:

3.1 The radio environment

The multiple channels of the receivers will allow studies of the natural and man-made radio background as a function of polarization. Vertical polarization is expected to contain more noise

than the horizontal polarizations, but this has not been quantified in Puerto Rico. This is important for the effective use of vector antennas, and for measurements of radio angular momentum, as discussed above, and will provide opportunities for student publications in professional journals. Graduate student projects could include the development of software to remove coupling effects between antennas and their surroundings, including nearby antennas and other nearby objects.

3.2 The radio sky

An intriguing project for both university and high school students is the use of the array as a radio telescope. The first radio astronomical observations were made by Karl Jansky at 20 MHz (Jansky, 1933), a frequency at which the array would commonly operate. Such a frequency in Puerto Rico may sometimes be impeded by the ionosphere during the daytime, but would be possible to use routinely at night.

3.3 Radio engineering

As noted above, using the alternative signal inputs of the receivers, radio frequencies of up to 400 MHz may be received, opening possibilities for many interesting projects for students of all levels in building antennas, filters, amplifiers and attenuators, firmware, and software, for special radar and radio projects. The differences between signals received on different antennas may be easily displayed, and the software-defined radio firmware of the receiving systems may be programmed to create a software radio which can detect and play radio stations received by the equipment, to aid in exploring the properties of electromagnetic waves and to learn about radio and communications technology.

4 Discussion and conclusion

The radio array described here will make significant contributions to ionospheric and radio research and development and related technical education. In addition to the array, a variety of supporting instruments will be fielded by project collaborators, including an optical imaging system; very-low-frequency (VLF) receivers; very-high-frequency (VHF) receivers and interferometers; global navigation satellite system (GNSS) scintillation and total electron content (TEC) receivers; lightning mapping arrays, interferometers, slow-field and fast-field antennas, and field mills; and a magnetometer.

Ionospheric radar and radio imaging in the high-frequency band will motivate the development of techniques to quantify and correct for radio propagation effects, including refraction and reflection near the critical plasma level. These techniques will be valuable whenever renewed radar observations of the solar corona might be performed using VHF radar imaging at the critical plasma level in the corona (James, 1970; Hysell et al., 2019).

Although the collapse of the Arecibo radar and radio telescope instrument platform on December 1, 2020, destroyed the primary and secondary reflectors required for the Arecibo high-power HF system, many other Arecibo instruments continue to operate, and it is hoped that the HF antenna system can be replaced, and the HF transmitting system restored to operation, in the near future. Along with instrumentation operating in Puerto Rico on Culebra Island, in Cayey, and at Arecibo, the radio array and other instruments deployed in Aguadilla will contribute to the continuation of the advances in atmospheric, geospace, and space research that Puerto Rico has been known for since the first observations at Arecibo Observatory on November 1, 1963.

Data availability statement

The original contributions presented in the study are included in the article. Further inquiries can be directed to the corresponding author.

Author contributions

BI developed the concepts and methods and wrote the paper. TB participated in developing the project. BG and EP developed methods and performed array calculations. CB and CF contributed ideas, strategies, and science goals. VB, FP-R, LN, AS, and MBÖ contributed science goals and methods. All authors contributed to the article and approved the submitted version.

Funding

The participation of BI was supported in part by U.S. National Science Foundation awards AGS-1428596 and AGS-1618691, by U.S. Army Research Office awards W911-NF-19-1-0486 and W911-NF-22-1-0144, and by Interamerican University of Puerto Rico. EP acknowledges support for basic research from U.S. Naval Research Laboratory 6.1 base funding. CB acknowledges support from U.S. National Science Foundation awards AGS-2221770 and AST-1744119.

Acknowledgments

The authors are grateful to Antonio Arias, Víctor Barreto-López, Víctor Barreto-Santos, Paul Bernhardt, Jorge Chau, Edwin Crespo-Cuevas, Michael Davis, Garred Giles, Richard Grubb, Linnea Kirby, Robert Livingston, Thomas Leyser, José López-Morales, Thomas Luker, Justin Mabie, Rafael Narváez-Martínez, José Ocasio-Manzano, Javier Quintana-Méndez, Francisco Reyes-Rodríguez, Michael Rietveld, Sergey Sergienko, Juha Vierinen, Nikolay Zabotin, and Gebreab Zewdie, for scientific and technical contributions, and to Élie Agésilas, Theresa Ahlin, Israel Ayala, Amaury Boscio-Vargas, Nataliya Byelyey, José Cabán, Rafael Canales-Pastrana, Peter Chatt, Nydia Feliciano-Burgos, José Fuentes-Meléndez, Rubén Hernández Jr., Patrick Giniewski, Monica Larson, Robert Livingston, Miguel López-Meléndez, Juan Martínez, Jessica Matthews, Robert McCoy, Carlos Olivares-Pacheco, Javier Quintana-Méndez, Edwin Rivera-Cordero, Anthony Rivera-González, Gilberto Rivera-Rosario, Serafín Rivera-Torres, Armando Rodríguez-Durán, Rafael Salgado-Mangual, Ingrid Silfa-Báez, Rose Annette

Suárez-Lucena, Roman Szymanski, Abel Vale-Nieves, and John Way, for administrative and logistical contributions.

Conflict of interest

The authors declare that the research was conducted in the absence of any commercial or financial relationships that could be construed as a potential conflict of interest.

Publisher's note

References

Bertoni, F., Batista, I. S., Abdu, M. A., Reinisch, B. W., and Kherani, E. A. (2006). A comparison of ionospheric vertical drift velocities measured by Digisonde and incoherent scatter radar at the magnetic equator. *J. Atmos. Solar-Terrestrial Phys.* 68, 669–678. doi:10.1016/j.jastp.2006.01.002

Blagoveshchenskaya, N. F., Kornienko, V. A., Rietveld, M. T., Thidé, B., Brekke, A., Moskvin, I. V., et al. (1998). Stimulated emissions around second harmonic of Tromsø heater frequency observed by long-distance diagnostic HF tools. *Geophys. Res. Lett.* 25, 873–876. doi:10.1029/98GL00492

Booker, H. G., Jing-Wei, T., and Behroozi-Toosi, A. B. (1987). A scintillation theory of fading in long-distance HF ionospheric communications. *J. Atmos. Terr. Phys.* 49 (9), 939–958. doi:10.1016/0021-9169(87)90006-7

Booker, H. G., and Tao, J.-W. (1987). A scintillation theory of the fading of HF waves returned from the F region: Receiver near transmitter. *J. Atmos. Terr. Phys.* 49, 915–938. doi:10.1016/0021-9169(87)90005-5

Carozzi, T., Thidé, B., Leyser, T. B., Komrakov, G., Frolov, V., Grach, S., et al. (2001). Full polarimetry measurements of stimulated electromagnetic emissions: First results. *J. Geophys. Res.* 106, 21395–21407. doi:10.1029/2001JA900004

Cheung, P. Y., Sulzer, M. P., DuBois, D. F., and Russell, D. A. (2001). High-power high-frequency-induced Langmuir turbulence in the smooth ionosphere at Arecibo, II: Low duty cycle, altitude-resolved, observations. *Phys. Plasmas* 8 (3), 802–812. doi:10.1063/1.1345704

Cheung, P. Y., Wong, A. Y., Pau, J., and Mjølhus, E. (1998). Controlled ionospheric preconditioning and stimulated electromagnetic radiation. *Phys. Rev. Lett.* 80, 4891–4894. doi:10.1103/PhysRevLett.80.4891

Chilson, P. B., Ulbrich, C. W., Larsen, M. F., Perillat, P., and Keener, J. E. (1993). Observations of a tropical thunderstorm using a vertically pointing, dual-frequency, collinear beam Doppler radar. *J. Atmos. Ocean. Tech.* 10 (5), 663–673. doi:10.1175/1520-0426(1993)010<0663:OOATTU>2.0.CO;2

Derblom, H., Thidé, B., Leyser, T. B., Nordling, J. A., Hedberg, Å., Stubbe, P., et al. (1989). Tromsø heating experiments: Stimulated emission at HF pump harmonic and subharmonic frequencies. *J. Geophys. Res. Space Phys.* 94 (A8), 10111–10120. doi:10.1029/JA094iA08p10111

DuBois, D. F., Russell, D. A., Cheung, P. Y., and Sulzer, M. P. (2001). High-power high-frequency-induced Langmuir turbulence in the smooth ionosphere at Arecibo, I: Theoretical predictions for altitude-resolved plasma line radar spectra. *Phys. Plasmas* 8 (3), 791–801. doi:10.1063/1.1345703

DuBois, D. (2000). "New directions in theory and experiment for HF excitation of Langmuir turbulence in the ionosphere," in 20th Anniversary Symposium on Ionospheric Interactions, Tromsø, Norway, October 2000.

DuBois, D., Vu, H. X., and Russell, D. (2011). "Electron acceleration in strong Langmuir turbulence: Exploiting the synergy of HF parametric excitation in the ionosphere and laser-induced parametric excitation," in RF Ionospheric Interactions Workshop, Santa Fe, NM, United States, April 2011.

Eliasson, B., Senior, A., Rietveld, M., Phelps, A. D. R., Cairns, R. A., Ronald, K., et al. (2021). Controlled beat-wave Brillouin scattering in the ionosphere. *Nat. Commun.* 12, 6209. doi:10.1038/s41467-021-26305-9

Eliasson, B., Shao, X., Milikh, G., Mishin, E. V., and Papadopoulos, K. (2012). Numerical modeling of artificial ionospheric layers driven by high-power HF heating. *J. Geophys. Res. (Space Phys.* 117 (A10), A10321. doi:10.1029/2012JA018105

Ferguson, D. C., Breakall, J. K., Bernhardt, P. A., Fernandez, F., Brum, C., Santoni-Ruiz, I., et al. (2022). A preliminary plan to quickly restore utility to the Arecibo 305-m telescope. *J. Astronomical Instrum.* 11 (3), 2250012–2250047. doi:10.1142/S225117172250012X

Garnung, M. B., Celestin, S., and Farges, T. (2021). HF-VHF electromagnetic emissions from collisions of sprite streamers. *J. Geophys. Res. (Space Phys.* 126 (6), e28824. doi:10.1029/2020JA028824

Grach, S. M., Sergeev, E. N., Mishin, E. V., and Shindin, A. V. (2016). Dynamic properties of ionospheric plasma turbulence driven by high-power high-frequency radiowaves. *Physics-Uspekhi* 59 (11), 1189–1228. doi:10.3367/UFNr.2016.07.037868

Grubb, R. N., Livingston, R., and Bullett, T. W. (2008). "A new general purpose high performance HF radar," in Proceedings of the URSI General Assembly, Chicago, IL, United States, 7-16 August 2008.

Hare, B. M., Scholten, O., Bonardi, A., Buitink, S., Corstanje, A., Ebert, U., et al. (2018). LOFAR lightning imaging: Mapping lightning with nanosecond precision. *J. Geophys. Res. Atmos.* 123, 2861–2876. doi:10.1002/2017JD028132

Henderson, B. S., Sultan, P. J., Sulzer, M. P., and Levine, E. V. (2022). High-resolution observation of heater-induced daytime plasma fluctuations at Arecibo. *J. Geophys. Res. Space Phys.* 127 (11), e2022JA030699. doi:10.1029/2022JA030699

Holden, D. N., Ulbrich, C. W., Larsen, M. F., Rottger, J., Ierkic, H. M., and Swartz, W. (1986). UHF and VHF radar observations of thunderstorms. *Handb. MAP* 20, 288–292.

Hysell, D. L., Chau, J. L., Coles, W. A., Milla, M. A., Obenberger, K., and Vierinen, J. (2019). The case for combining a large low-band very high frequency transmitter with multiple receiving arrays for geospace research: A geospace radar. *Radio Sci.* 54 (7), 533–551. doi:10.1029/2018RS006688

Isham, B., Hagfors, T., Khudukon, B., Yurik, R., Tereshchenko, E. D., Rietveld, M. T., et al. (2005). An interferometer experiment to explore the aspect angle dependence of stimulated electromagnetic emission spectra. *Ann. Geophys.* 23, 55–74. doi:10.5194/angeo-23-55-2005

Isham, B., Tepley, C. A., Sulzer, M. P., Zhou, Q. H., Kelley, M. C., Friedman, J. S., et al. (2000). Upper atmospheric observations at the Arecibo Observatory: Examples obtained using new capabilities. *J. Geophys. Res.* 105 (A8), 18609–18637. doi:10.1029/1999JA900315

James, J. C. (1970). Some observed characteristics of solar radar echoes and their implications. *Sol. Phys.* 12 (1), 143–162. doi:10.1007/BF02276574

Jansky, K. G. (1933). Radio waves from outside the solar system. *Nature* 132 (3323), 66. doi:10.1038/132066a0

Karashtin, A. N., Korobkov, I. S., Frolov, V. L., and Tsimring, M. S. (1986). Stimulated radio emission of the ionospheric plasma at the second harmonic of the pump wave frequency. *Radiophys. Quant. Elec.* 29, 22–25. doi:10.1007/BF01033998

Kruer, W. L. (1990). Simulations of electromagnetic wave plasma interactions. *Radio Sci.* 25 (6), 1351–1357. doi:10.1029/RS025i006p01351

LaBelle, J. (2012). First observations of $5f_{ce}$ auroral roars. *Geophys. Res. Lett.* 39, L19106. doi:10.1029/2012GL053551

LaBelle, J., and Treumann, R. A. (2002). Auroral radio emissions, 1: Hisses, roars, and bursts. *Space Sci. Rev.* 101 (3), 295–440. doi:10.1023/A:1020850022070

Leyser, T. B., Norin, L., McCarrick, M., Pedersen, T. R., and Gustavsson, B. (2009). Radio pumping of ionospheric plasma with orbital angular momentum. *Phys. Rev. Lett.* 102, 065004. doi:10.1103/PhysRevLett.102.065004

Leyser, T. B. (2001). Stimulated electromagnetic emissions by high-frequency electromagnetic pumping of the ionospheric plasma. *Space Sci. Rev.* 98 (3), 223–328. doi:10.1023/A:1013875603938

Mahmoudian, A., Nossa, E., Isham, B., Bernhardt, P. A., Briczinski, S. J., and Sulzer, M. (2019). NSEE yielding electron temperature measurements at the Arecibo Observatory. *J. Geophys. Res. Space Phys.* 124 (5), 3699–3708. doi:10.1029/2019JA026594

McKay, D., Fallows, R., Norden, M., Aikio, A., Vierinen, J., Honary, F., et al. (2015). All-sky interferometric riometry. *Radio Sci.* 50 (10), 1050–1061. doi:10.1002/2015RS005709

Meyer, J., and Zhu, Y. (1993). Measurement of two plasmon decay instability development in k space of a laser produced plasma and its relation to 3/2-harmonic generation. *Phys. Rev. Lett.* 71, 2915–2918. doi:10.1103/PhysRevLett.71.2915

Meyer, M. G., and Sahr, J. D. (2004). Passive coherent scatter radar interferometer implementation, observations, and analysis. *Radio Sci.* 39 (3). doi:10.1029/2003RS002985

Mir, H. S., and Sahr, J. D. (2007). Passive direction finding using airborne vector sensors in the presence of manifold perturbations. *IEEE Trans. Signal Process.* 55 (1), 156–164. doi:10.1109/TSP.2006.882056

Mjølhus, E. (1998). Theoretical model for long time stimulated electromagnetic emission generation in ionospheric radio modification experiments. *J. Geophys. Res. Space Phys.* 103 (A7), 14,711–14,729. doi:10.1029/98JA00927

Mohammadi, S. M., Daldorff, L. K. S., Bergman, J. E. S., Karlsson, R. L., Thide, B., Forozesh, K., et al. (2010a). Orbital angular momentum in radio: A system study. *IEEE Trans. Antennas Propag.* 58 (2), 565–572. doi:10.1109/TAP.2009.2037701

Mohammadi, S. M., Daldorff, L. K. S., Forozesh, K., Thidé, B., Bergman, J. E. S., Isham, B., et al. (2010b). Orbital angular momentum in radio: Measurement methods. *Radio Sci.* 45 (4). doi:10.1029/2009RS004299

Obenberger, K. S., Dowell, J. D., Malins, J. B., Parris, R., Pedersen, T., and Taylor, G. B. (2018). Using lightning as a HF signal source to produce ionograms. *Radio Sci.* 53, 1419–1425. doi:10.1029/2018RS006680

Obenberger, K. S., Holmes, J. M., Ard, S. G., Dowell, J., Shuman, N. S., Taylor, G. B., et al. (2020). Association between meteor radio afterglows and optical persistent trains. *J. Geophys. Res. Space Phys.* 125 (9), e2020JA028053. doi:10.1029/2020JA028053

Paznukhov, V. V., Galushko, V. G., and Reinisch, B. W. (2012). Digisonde observations of tids with frequency and angular sounding technique. *Adv. Space Res.* 49 (4), 700–710. doi:10.1016/j.asr.2011.11.012

Reinisch, B., Huang, X., Galkin, I., Paznukhov, V., and Kozlov, A. (2005). Recent advances in real-time analysis of ionograms and ionospheric drift measurements with digisondes. *J. Atmos. Solar-Terrestrial Phys.* 67 (12), 1054–1062. doi:10.1016/j.jastp.2005.01.009

Reinisch, B. W., Galkin, I. A., Khmyrov, G. M., Kozlov, A. V., Bibl, K., Lisysyan, I. A., et al. (2009). New digisonde for research and monitoring applications. *Radio Sci.* 44 (1). doi:10.1029/2008RS004115

Rietveld, M., Kohl, H., Kopka, H., and Stubbe, P. (1993). Introduction to ionospheric heating at Tromsø, I: Experimental overview. *J. Atmos. Terr. Phys.* 55 (4), 577–599. doi:10.1016/0021-9169(93)90007-L

Russell, D. A., and DuBois, D. F. (2001). 3/2 ω_0 radiation from the laser-driven two-plasmon decay instability in an inhomogeneous plasma. *Phys. Rev. Lett.* 86 (3), 428–431. doi:10.1103/PhysRevLett.86.428

Sedgemore, K. J. F., Wright, J. W., Williams, P. J. S., Jones, G. O. L., and Rietveld, M. T. (1998). Plasma drift estimates from the Dynasonde: Comparison with EISCAT measurements. *Ann. Geophys.* 16 (10), 1138–1143. doi:10.1007/s00585-998-1138-y

Sergeev, E., Grach, S., Shindin, A., Mishin, E., Bernhardt, P., Briczinski, S., et al. (2013). Artificial ionospheric layers during pump frequency stepping near the 4th gyroharmonic at HAARP. *Phys. Rev. Lett.* 110, 065002. doi:10.1103/PhysRevLett.110.065002

Stock, M. G., Akita, M., Krehbiel, P. R., Rison, W., Edens, H. E., Kawasaki, Z., et al. (2014). Continuous broadband digital interferometry of lightning using a generalized cross-correlation algorithm. *J. Geophys. Res. Atmos.* 119 (6), 3134–3165. doi:10.1002/2013JD020217

Streltsov, A. V., Berthelier, J. J., Chernyshov, A. A., Frolov, V. L., Honary, F., Kosch, M. J., et al. (2018). Past, present and future of active radio frequency experiments in space. *Space Sci. Rev.* 214 (8), 118. doi:10.1007/s11214-018-0549-7

Tereshchenko, E. D., Yurik, R. Y., Khudukon, B. Z., Rietveld, M. T., Isham, B., Belyey, V., et al. (2006). Directional features of the downshifted peak observed in HF-induced stimulated electromagnetic emission spectra obtained using an interferometer. *Ann. Geophys.* 24 (7), 1819–1827. doi:10.5194/angeo-24-1819-2006

Thidé, B., Djuth, F. T., Leyser, T. B., and Ierkic, H. M. (1995). Evolution of Langmuir turbulence and stimulated electromagnetic emissions excited with a 3-MHz pump wave at Arecibo. *J. Geophys. Res.* 100 (23), 23887–23923. doi:10.1029/95JA01631

Thidé, B., Hedberg, Å., Fejer, J. A., and Sulzer, M. P. (1989). First observations of stimulated electromagnetic emission at Arecibo. *Geophys. Res. Lett.* 16 (5), 369–372. doi:10.1029/GL016i005p00369

Thidé, B., Kopka, H., and Stubbe, P. (1982). Observations of stimulated scattering of a strong high-frequency radio wave in the ionosphere. *Phys. Rev. Lett.* 49, 1561–1564. doi:10.1103/PhysRevLett.49.1561

Thidé, B., Then, H., Sjöholm, J., Palmer, K., Bergman, J., Carozzi, T. D., et al. (2007). Utilization of photon orbital angular momentum in the low-frequency radio domain. *Phys. Rev. Lett.* 99 (8), 087701701. doi:10.1103/PhysRevLett.99.087701

Vertatschitsch, L. (2013). *High bandwidth, multi-purpose passive radar receiver design for aerospace and geoscience targets,* PhD thesis. Seattle, WA, United States: University of Washington.

Wright, J. W., Paul, A. K., and Pitteway, M. L. V. (1980). On the accuracy and interpretation of Dynasonde virtual height measurements. *Radio Sci.* 15, 617–626. doi:10.1029/RS015i003p00617

Wright, J. W., and Pitteway, M. L. V. (1979). Real-time data acquisition and interpretation capabilities of the Dynasonde: 1. Data acquisition and real-time display. *Radio Sci.* 14, 815–825. doi:10.1029/RS014i005p00815

Yampolski, Y., Milikh, G., Zalizovski, A., Koloskov, A., Reznichenko, A., Nossa, E., et al. (2019). Ionospheric non-linear effects observed during very-long-distance HF propagation. *Front. Astronomy Space Sci.* 6. doi:10.3389/fspas.2019.00012

Zabotin, N. A., Godin, O. A., and Bullett, T. W. (2016). Oceans are a major source of waves in the thermosphere. *J. Geophys. Res. Space Phys.* 121 (4), 3452–3463. doi:10.1002/2016JA022357

Zabotin, N. A., Wright, J. W., and Zhbankov, G. A. (2006). NeXtYZ: Three-dimensional electron density inversion for Dynasonde ionograms. *Radio Sci.* 41, RS6S32. doi:10.1029/2005RS003352